Mon. Not. R. Astron. Soc. **000**, 000–000 (0000) Printed 1 July 2004 (MN LaTeX style file v2.2)

Optical Spectroscopy of X-Mega targets - V. FO 15 : a new early O-Type double-lined binary in the Carina Nebula

N.I. Morrell[1]*, J.F. Albacete Colombo[2]†, V. S. Niemela[2]‡, R. Barbá[3]§, M. Orellana[4]¶,
[1] *Las Campanas Observatory, Observatories of the Carnegie Institution of Washington, Casilla 601, La Serena, Chile.*
[2] *Facultad de Ciencias Astronómicas y Geofísicas de la La Plata, Paseo del Bosque S/N, 1900 La Plata, Argentina.*
[3] *Departamento de Física y Astronomía, Universidad de La Serena, Chile.*
[4] *Instituto Argentino de Radioastronomía, Villa Elisa, Argentina.*

1 July 2004

ABSTRACT

We present optical spectroscopy of the O-type star FO 15 , a member of the open cluster Trumpler 16 in the Carina Nebula (NGC 3372), showing that this is a double-lined close binary system. We have obtained a radial velocity orbit for this binary finding a circular solution with a period of 1.41358 $\pm$ 0.00001 days and semi-amplitudes of 229 $\pm$ 2 km s^{-1} and 436 $\pm$ 3 km s^{-1} for the primary and secondary components, yielding minimum masses of 28 $\pm$ 1 and 15 $\pm$ 1 M$_{\odot}$, respectively. We classify the primary spectrum as O5 V((f)), and the secondary as O9.5 V. High resolution spectroscopy of FO 15 is used to derive the luminosity ratio for the system components, and the corresponding values of the projected rotational velocities. This information, together with magnitudes and colors from the literature and the assumpion of synchronous rotation, allows estimation of physical parameters for the binary components. This is done for different values of the total to selective absorpion ratio R, finding that a value of R around 4.1 can be appropriate for this star. ¿From the analysis of XMM-Newton observations we find that the X-ray emission originated in FO 15 shows strong variations and can be represented by a two temperature model with kT$_1$ = 0.16 and kT$_2$ = 2.7 keV, respectively, revealing FO 15 as a hard X-ray source. Furthermore, the unabsorbed luminosity ratio L$_{\rm x}$/L$_{\rm bol}$ is significantly larger than observed in most single O-type stars. This behavior is probably due to wind collision between the hot massive components of this short period binary.

Key words: binaries: general - open clusters and associations: individual: Trumpler 16 - stars: early-type - stars: fundamental parameters - stars: individual: FO 15 - X-rays: stars

1 INTRODUCTION

The Carina Nebula region (NGC 3372) contains one of the larger concentrations of OB stars known in our Galaxy. Some of the bright open clusters that constitute its stellar population are known by their high content of O-type stars (this is the case of Trumpler 14 and Trumpler 16). Many early-type stars are also found between the less conspicuous ones, lying in more obscured regions, as several stars classified as OB$^+$ in an objective prism study carried out by Forte & Orsatti (1981). These authors called the attention on the star identified with # 15 (hereafter FO 15 , $\alpha_{2000} = 10^{\rm h}45^{\rm m}36^{\rm s}$; $\delta_{2000} = -59^{\circ}48'22''$; V = 12.05) to which they assigned the spectral type O4V, based on a spectrogram obtained at the CTIO 1-m telescope with the CITS (Carnegie Image-Tube Spectrograph), at a reciprocal dispersion of 43 Å mm^{-1}. Also, from the analysis of their photoelectric photometry, these authors stated that the star presents a high reddening and possible photometric variations, obtaining for it a value of B-V = 0.86, U-B = -0.20 with an accuracy estimated in $\pm$ 0.02 mag.

In more recent bibliography we found CCD photome-

* Member of Carrera del Investigador Científico, CONICET, on leave from Facultad de Ciencias Astronómicas y Geofísicas de La Plata, Argentina.
† Post-doctoral fellow of CONICET, Argentina.
‡ Member of Carrera del Investigador, CIC, Provincia de Buenos Aires, Argentina.
§ Member of Carrera del Investigador Científico, CONICET, on leave from Facultad de Ciencias Astronómicas y Geofísicas de La Plata, Argentina.
¶ Student fellow of CIC Prov. de Buenos Aires, Argentina

try of FO15, obtained by Massey & Johnson (1993) in their study of massive stars near η Carina. In this paper the star is identified with the number 596, and its corresponding photometric measurements are: V = 12.10, U-B = 0.04, and B-V = 0.60. The estimated errors in this case are $\pm$ 0.03 mag in V, $\pm$ 0.03 mag in B, and $\pm$ 0.05 mag in U. The discrepancy in the B-V color between Massey & Johnson (1993) and Forte & Orsatti (1981) is not very surprising, considering that the star lies in a highly obscured region of the nebula, namely the V-shaped dust lane South of Eta Carinae. In this kind of regions, considerable differences between photoelectric and CCD measurements are often found. The intrinsic photometric variability of the object is another possible source of discrepant measurements of magnitudes and colors.

In view of its early spectral type, and the suspected presence of light variations, we thought FO 15 deserved to be included in our on-going search for massive binary systems in the Carina Nebula. The fact that the star is surrounded by dense interstellar material, as evidenced by its high reddening, might also be an indication of its extreme youth, thus increasing the interest in determining its binary status.

It is well known the scarcity of early O-type binary systems for which an orbital solution is available. Also known are the differences between the masses estimated from the comparison of stellar luminosities with evolutionary models, and those inferred from studies of binary systems (see, e.g. Herrero et al. 1992 and Herrero, Puls & Villamariz 2000, for a more recent revision of the problem). One way to help in clarifying this situation, is through the discovery and subsequent study of non evolved massive binary systems, like the one here presented.

FO 15 was discovered as an X-ray source on EINSTEIN observations of the Carina Nebula, published in the X-ray catalog of O-type stars by Chlebowski et al. (1989). Such study is based on Imaging Proportional Counter (IPC) and High Resolution Imager (HRI) observations in the (0.2–3.5) keV energy range. In that work, the authors supposed a distance of 3900 pc to FO 15 and calculated a maximum value for the luminosity of 17.4×10^{32} erg s^{-1} ($f_x \leq 9.5 \times 10^{-13}$ erg s^{-1} cm^{-2}). If a distance of 2250 pc (now frequently adopted for the O-type stars in Tr 16) is assumed, the observed X-ray flux leads to a luminosity upper limit of 5.8×10^{32} erg s^{-1}. This value is in rough agreement with our present estimation reported in section 5.

FO 15 was also observed by the ROSAT satellite in the context of the X-Mega international campaign (Corcoran 1996), which also involves spectroscopic observations of hot stars with detectable X-ray emission. The ROSAT-HRI image shows a weak X-ray emission at the FO 15 position, considerably lower than that detected in the first EINSTEIN observation of this star. Also, FO 15 is present as a hard X-ray source in XMM-Newton observations of the Carina Nebula (Albacete Colombo et al. 2003).

We decided to conduct an optical and X-ray study of FO 15 in order to establish its binary status, physical parameters, and the origin of the detected X-ray emission of this star.

2 OBSERVATIONS

2.1 Optical spectroscopy

Twenty five spectral images of FO15 were obtained with the 2.15-m telescope at Complejo Astronómico El Leoncito (CASLEO)[1] in San Juan, Argentina, during several observing runs held between February 1996 and March 2003.

We used, alternatively, the Cassegrain Boller & Chivens (B&C) spectrograph, with a 600 l mm^{-1} grating and a PM 516×516 20μm pixel CCD as detector, and the REOSC spectrograph, in its Simple Dispersion mode. For the REOSC spectra a TEK 1024×1024 pixel CCD, with pixel size of 24μm was used as detector. This instrumental configurations provide reciprocal dispersions of ~2.3 and 2.0 Å px^{-1}, respectively. The wavelength region observed was roughly $\lambda\lambda$3900 – 5040 Å.

We used a slit width of 2 arcsec for all our CASLEO spectra. Exposure times for the stellar images ranged between 30 minutes and 1 hour, resulting in spectra of signal-to-noise ratio between 50 and 150, depending on seeing and transparency. He-Ar and Cu-Ar comparison arc images were observed with the B&C and REOSC spectrographs, respectively, at the same telescope position as the stellar images immediately after or before the stellar exposures. The usual series of bias and flat-field frames were also obtained for each observing night.

One high resolution spectroscopic observation of FO 15 was obtained with ESO-VLT UT2 (Kueyen) and the UV-Visual Echelle Spectrograph (UVES) in December 2001. The setting used produced a blue spectrum covering the region 3260-4520Å with a resolution (2 pixels) R = 67000 and a red one spanning from 4580 to 6690Å at a spectral resolution (2 pixels) R = 58000. High gain, 2 × 2 binning mode was used. A signal-to-noise of ~50 was achieved in this observation.

Three high resolution spectra were obtained at Las Campanas Observatory (LCO), as follows: one in December 2002, with the Magellan II (Clay) 6.5-m telescope and Magellan Inamori Kyocera Echelle (MIKE) double echelle spectrograph (Bernstein et al. 2003). A 1 × 3 binning was applied achieving a resolution of 19000 in the red spectrum (4500 - 7200 Å) and 29000 in the blue spectrum (3200-4700 Å), at a signal-to-noise ranging from 60 to 200 in the red and from 40 to 100 in the blue in a 1200 s exposure using a 1 arcsec width slit. Another echelle observation was obtained in May 2003 with the Magellan I (Baade) 6.5-m telescope and MIKE. No binning was applied to these data yielding a resolution $R \sim 36000$ in the blue spectrum (3200 - 4800Å) and 27000 in the red spectrum (4800 - 8800Å), with a 0.7 arcsec width slit. The signal-to-noise achieved in the 600 seconds exposure is 60-130 in the red spectrum and 10-60 in the blue spectrum. A third echelle spectrum of FO 15 was obtained with the 2.5-du Pont telescope and its echelle sepctrograph in July 2003. The signal-to-noise achieved in the 3 × 1200 seconds exposure ranges from 10 to 140 from the blue (3700 Å) to the red end (10000 Å) of the spectrum at a resolution $R \sim 23000$ using a 0.75 arcsec slit.

Th-Ar comparison lamps were secured for every high

[1] CASLEO is operated under agreement between CONICET, SeCyT, and the Universities of La Plata, Córdoba and San Juan, Argentina

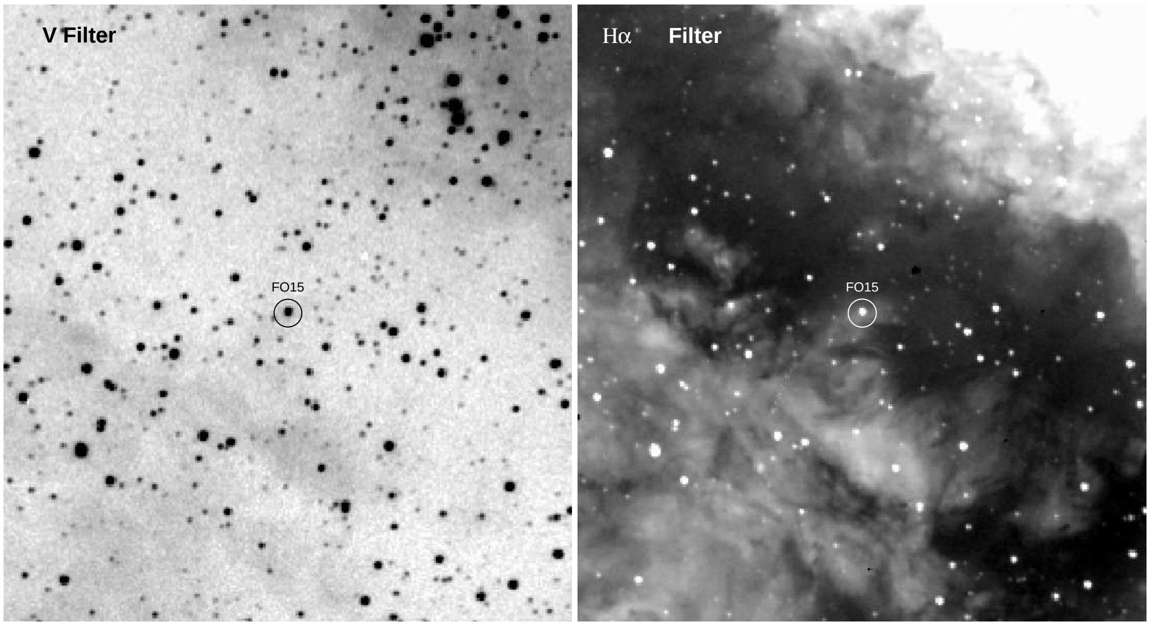

Figure 1. Images obtained in May 1999 at the CTIO Curtis-Schmidt Telescope using V and Hα filters, respectively.

resolution observation as well as the usual series of bias and flat-field exposures.

All the spectroscopic data were processed and analyzed with standard IRAF routines. MIKE spectra were extracted using the IRAF tasks contained in the *mtools* package, developed by J. Baldwin and available for downloading from LCO website.

2.2 X-ray observations

The Carina Nebula was also observed in X-ray energies with the XMM-Newton satellite in five separate revolutions, two of them available for analysis in this paper. The observatory consists of three X-ray telescopes and the data were acquired with the European Photon Imaging Camera (EPIC), which provides simultaneous CCD imaging-timing-spectroscopy from the PN camera (Strüder 2001) and two identical MOS cameras, MOS-1 and MOS-2 (Turner 2001). Thick blocking filters were used in order to reject optical and ultraviolet light. These two conditions apply only to the PN and MOS-1 cameras, which provide a field of view of $\approx$ 30' in diameter and energy coverage from $\approx$ 0.2 to 15 keV at medium energy resolution ($E/\Delta E \approx$ *20–50*) and $\approx$12" FWHM angular resolution.

All data sets were retrieved from the public XMM-Newton data archive XSA [2] (see Table 1).

3 OPTICAL ANALYSIS

3.1 Spectral classification of FO15

Applying the classification criteria specified by Walborn & Fitzpatrick (1990) to our low resolution observations, we obtained for FO 15 the spectral type O5V. Later, once we had derived the orbital parameters, we focused the analysis on the spectral behavior over the orbital motion and then we noted that the relative intensities between He II λ4542Å and He I λ4471Å absorptions, whose ratio is used as temperature indicator, change with orbital phase, then affecting the derived spectral classification. One of our low resolution observations of FO 15 is illustrated in Figure 2.

From our set of CASLEO spectra, we decided to use for spectral classification the observations with larger radial velocity separation between components. The relative intensities of He II λ4542Å and He I λ4471Å absorptions, as observed in our data, compared to the O-type standards presented by Walborn & Fitzpatrick (1990), seem to be close to the spectral type O5V for the primary binary component, slightly later than the former classification by Forte & Orsatti (1981). Regarding the secondary component, while the signal-to-noise of our low resolution data does not allow a precise classification, we determined a spectral type near O9V, because its presence is detected only in He I and H lines, with no signs of doubling in the He II absorptions, which means that they are either absent or diluted by effect of the primary star continuum.

Once the high resolution spectra were available, we measured equivalent widths of the He I and He II lines on the obsevations showing larger radial velocity differences between components. We then applied to those measurements the classification criteria described by Conti (1973) and Kerton & Martin (1999) to compare the equivalent widths of He I 4471 vs. He II 4542 and He I 4922 vs. He II 5411, respectively. The He II lines corresponding to the secondary component are barely visible on the high resolution observations. Also in the echelle data we can distinguish the presence of weak λ 4634-4640-4642 N III emission from the primary component, then identifying it as an O5V((f)). According to these criteria, we obtained for the primary and secondary components of FO 15 spectral classifications of O5V((f)) and O9.5V, respectively. Variations of half spectral class on both

[2] http://xmm.vilspa.esa.es/xsa

Table 1. X-ray observing log.

Rev.	Central	Observation	HJD [days]	Observation in Y/M/D at H:M:S (UTC)		Exposure†	Observing
N°	Target	Id.	2400000+	Start time	End time	Time (sec)	Mode
115	η Carina	0112580601	51751.741	2000/07/26 at 04:59:20	2000/07/26 at 15:07:49	32000	PFF-PPSF
116	η Carina	0112580701	51753.526	2000/07/27 at 23:49:25	2000/07/28 at 03:16:30	9800	PFF-PPSF

Note: † Exposure times expressed as averages. Individual exposures for MOS1, MOS2, PN are slightly different. Heliocentric Julian Dates (HJD) were calculated at the exposure start time. PPSF refer to Prime-Full-Frame and Prime-Partial-Small-Frame observing modes used in the different EPIC camera configurations.

components, probably related to the Struve-Sahade effect, may also be present.

According to this classification, FO 15 is the second earliest double-lined binary system studied in the Carina Nebula, following HD 93205 (O3.5V + O8V).

3.2 Radial velocities

From the first spectral images of FO 15 , obtained in successive nights, we noted the shift of the stellar Hβ absorption line, which changes position relative to the nebular Hβ emission. Then FO 15 appeared as a possible short period binary system. Radial velocities were determined for all the observed lines in our spectra of FO 15 fitting Gaussian profiles.

Because nebular emission is present in the spectrum of FO 15 (as seen in Figure 2), and it may affect the radial velocities derived from H and HeI absorptions, we decided to consider the absorption lines of He II as more representative of the radial velocity of the primary star in our low resolution spectra. As for the echelle data, both He II and He I lines were considered for the primary component, while the secondary velocities were derived from He I absorptions. In Table 2 we list the heliocentric radial velocities obtained from our observations of FO 15 along with the Heliocentric Julian Date (HJD) for each observation, labeled according to the corresponding observatory of origin and instrumental configuration (see notes to the table). For most of the low resolution observations, the radial velocities quoted in Table 2 are the average of three He II lines, namely 4200, 4542 and 4686 Å for the primary component, and only He I 4471 Å for the secondary. Several other He II and He I lines were measured on the echelle spectra. Rest wavelengths were taken from Bolton & Rogers (1978) tables.

From our low resolution spectra, we also obtained mean radial velocities for the nebular emission lines of [O III] λ4958.9 and λ 5006.86, being -33 $\pm$24 and -36 $\pm$20 respectively, consistent with the radial velocity of -19 $\pm$ 10 km s^{-1}, given by Grabelsky et al. (1988) from CO observations of the η Carina Nebula.

3.3 Orbital Period

From the radial velocities listed in Table 2, it was already apparent that the orbital period of FO 15 was of the order of a few days. Several period search algorithms: Lafler & Kinman (1965), Marraco & Muzzio (1980), and Cincotta et al. (1995) were applied independently to the observed radial velocities of each line with coincident results. We found periods of P= 1.4135$\pm$0.0001 days for He II λ4200 , P= 1.4133$\pm$0.0003 days for He II λ4541 and P= 1.4137$\pm$0.0002 for He II λ4686. As all of these periods coincide within the errors, and no alias periods with similar probabilities were found, we have adopted P = 1.4135 $\pm$ 0.0006 days as the most probable value of the orbital period of FO 15 . Further orbital fitting yield 1.41358 $\pm$ 0.00001 as the most probable value for this binary period, which is quoted in Table 3.

Table 2. Observed heliocentric radial velocities for the primary and secondary components of FO 15 . The orbital phases are relative to the time of maximum radial velocity of the primary. Radial velocities and (O-C) values are in [km s^{-1}].

HJD (days)	Phase	Primary		Secondary	
2400000+	ϕ	VR	O-C	VR	O-C
50125.751(a)	0.316	102	-24		
50127.747(a)	0.728	-4	43		
50128.758(a)	0.443	222	10	-361	79
50129.694(a)	0.105	-165	-7		
50471.804(a)	0.122	-180	-42		
50472.773(a)	0.808	-148	6		
50473.778(a)	0.519	204	7	-431	-19
50477.807(a)	0.369	167	-10		
50479.787(a)	0.770	-126	-20		
50854.825(a)	0.080	-211	-25		
50858.785(a)	0.882	-218	6	324	-32
50860.749(a)	0.271	-15	-85		
50861.739(a)	0.971	-247	2	426	22
51355.466(a)	0.246	18	-17		
51653.594(a)	0.148	-72	31		
51654.551(a)	0.825	-173	1		
51718.487(a)	0.055	-206	2	361	32
51959.799(a)	0.765	-109	-9		
51960.842(a)	0.503	199	-4	-452	-26
51961.765(a)	0.156	-76	17		
51962.776(a)	0.871	-210	6	369	26
52251.847(b)	0.367	179	3	-377	-3
52298.849(a)	0.617	106	0		
52302.856(a)	0.452	190	-22	-439	2
52329.604(a)	0.374	236	54	-346	37
52332.820(a)	0.649	44	-21		
52628.844(c)	0.063	-192	9	325	9
52690.606(a)	0.755	-113	26		
52766.626(c)	0.534	200	12	-399	-4
52836.495(d)	0.961	-225	25	420	15

Note: Data origin: (a) CASLEO, (b) ESO-VLT, (c) LCO-Magellan, (d) LCO-du Pont

3.4 Radial Velocity Orbit

We have determined the radial velocity orbit of FO 15 using a modified version of the code originally written by Bertiau & Grobben (1969).

We worked separately with the radial velocities of each HeII line, obtaining very similar, almost circular, orbital solutions. Thus we decided to use the average radial velocities in the following calculations. At last, we included the ra-

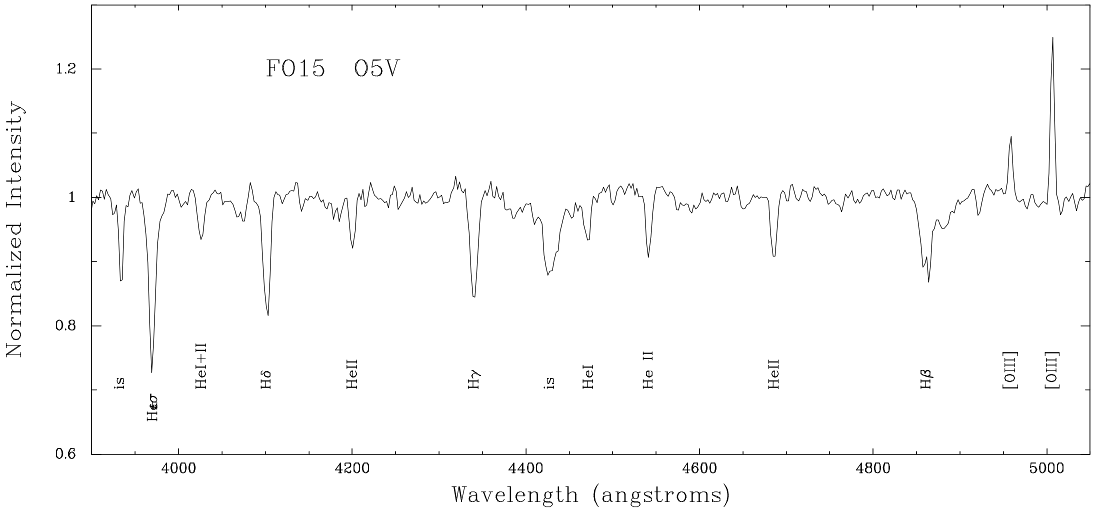

Figure 2. Normalized spectrum of FO 15 obtained at CASLEO, in February 1998.

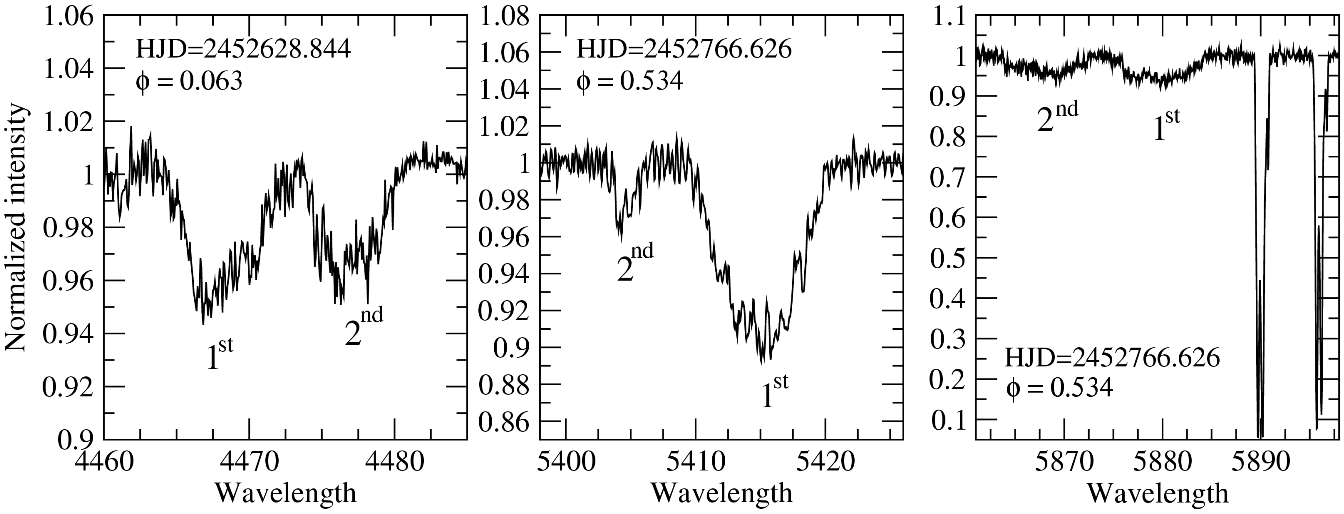

Figure 3. Normalized spectrum of FO 15 obtained at LCO with MIKE spectrograph, showing the primary and secondary components of the HeI 4471 (left), HeII 5411 (center) and HeI 5876 Å lines with the complex structure of the interstellar NaI lines (right), respectively.

dial velocities of the secondary star, and solved the orbit for the whole data set. We assigned weights of 5 to our high resolution observations while the lower resolution ones were weighted as 1 or 0.1 according to data quality (i.e. signal-to-noise ratio, moon contamination, etc.) and orbital phase (observations far from quadrature phases were assigned the lower weight). The resulting orbital parameters, are listed in Table 2, along with their corresponding standard errors.

Figure 4 represents the complete set of observed radial velocities as a function of the adopted orbital period, along with the circular orbital solution from Table 2.

Table 3. Orbital Elements of FO15

Parameters	Solution	Error
System		
P [days]	1.41358	0.00001
V_o [km s^{-1}]	-18	2
T_{vmax} [HDJ]	2450128.8	0.1
$q(M_1/M_2)$	0.55	0.01
Primary		
$a_1 \sin i$ [$R_\odot$]	6.46	0.09
K_1 [km s^{-1}]	231	3
$M_1 \sin^3 i$ [$M_\odot$]	28	1
Secondary		
$a_2 \sin i$ [$R_\odot$]	11.82	0.09
K_2 [km s^{-1}]	423	9
$M_2 \sin^3 i$ [$M_\odot$]	15	1

The Probable Error of the Fit is 14 km s^{-1}.

4 PHYSICAL PARAMETERS

One of the most intriguing problems of the Carina Nebula is its differential interstelar extinction law, which is produced by dense dust and gas structures that vary from place to place (Tapia et al. 1988, 2003). In Figure 1 we show that

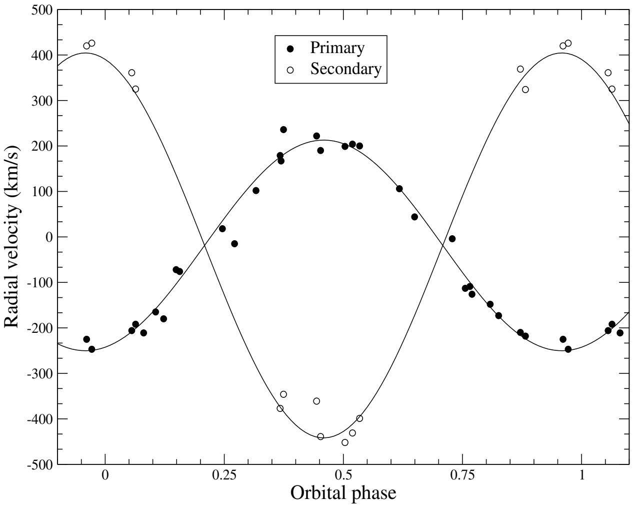

Figure 4. Average radial velocities from He IIλ4200, He IIλ4541 Å and He IIλ4686 Å absorption lines in the spectrum of FO 15 phased with the period of 1.41358 days. Continuous curves represent the orbital solutions from Table 2.

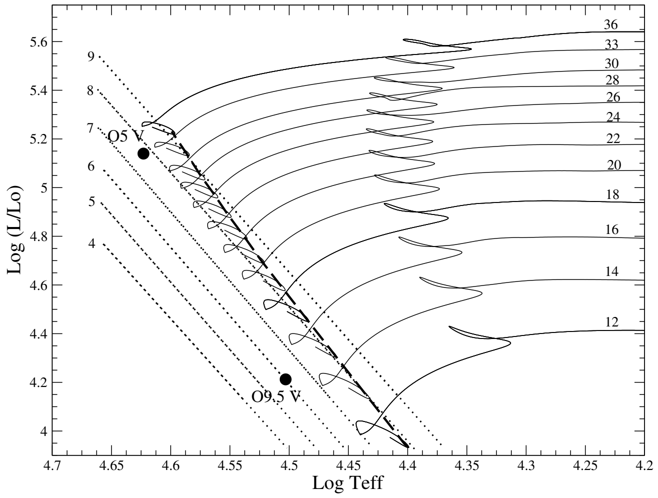

Figure 5. Position of the O5V((f)) and O9.5V components on the theoretical H-R diagram. Continuous lines represent evolutionary tracks from 12 to 36 $M_\odot$ labeled on the right with the mass of each model. Dotted lines are locii of constant radii labeled on the left with the radii in solar units. The thin dashed line represents the ZAMS isochrone. Model calculations provided by A.M. Serenelli (private communication).

FO 15 lies in the V-shaped dust and gas lane, that is characterized by anomalous values of $R = A_v/E_{B-V}$.

As FO 15 is a probable member of the Trumpler 16 cluster, we decided to adopt for this star the distance modulus of 11.76 ± 0.15 (2250 ± 180 pc), derived by Davidson et al. (2001) and then try different values of R, running from 3.2 to 4.1, in the derivation of the physical parameters of both FO 15 stellar components.

In order to determine the relative contribution of the primary (O5V((f))) and secondary (O9.5V) components to the total observed brightness of FO 15 we applied the corrected integrated absorption method described by Petrie (1940). We adopted for FO 15 a visual magnitude $V = 12.05$ and $(B\text{-}V) = 0.86$ from Forte & Orsatti (1981), $(B\text{-}V)_0 = -0.33$ from Schmidt-Kaler (1982). In the high resolution spectra we measured the equivalent widths of the HeI 4471 Å, and HeII 4542 and 4686 Å absorptions of the primary component, and HeI 4388 and 4471 Å of the scondary component, and compared those measurements after correction by the equivalent widths of the same lines in the spectra of single stars of similar spectral types obtained by Conti & Alschuler (1971) and Mathys (1988). In this way we obtained a luminosity ratio $l_2/l_1 = 0.24 \pm 0.04$ for the binary components of FO 15.

In table 4, we present the derived physical parameters for FO 15 (O5V((f))+O9.5V) using the spectral type vs. effective temperature ($T_{\rm eff}$) calibration from Markova et al. (2004). Furthermore, we used the bolometric corrections (BCs) from Howarth & Prinja (1989). We then adopted a $T^1_{\rm eff} = 42000$ K and $BC_1 = -3.86$ and $T^2_{\rm eff} = 31850$ K and $BC_2 = -3.04$ for the primary and secondary stars, respectively.

According to the expressions given by Zahn (1977), the synchronization time ($t_{\rm syn} \approx 5.3 \times 10^4$ years) for FO 15 is short enough to consider synchronous rotation as a good hypothesis for this system. We calculated the rotational broadening of the non-LTE HeI 4471 spectral line profile (Auer & Mihalas 1972) assuming $\log(g)$=4, and effective temperatures ($T_{\rm eff}$) of 40000 and 30000 K for the O5V((f)) and O9.5V components, respectively. Then, through comparison of the observed full width at half maximum of the HeI 4471 line in our high resolution spectra with the rotationally broadened numerical profiles, we estimated projected rotational velocities ($V \sin i$) of 240 and 150 km s^{-1}, for the primary and secondary components of FO 15, respectively.

Current analysis of photometric observations of FO 15 (Fernández-Lajús et al. in preparation) yields a lower limit for the inclination of the orbital plane of 70°. In this case, the absolute masses and radii of the FO 15 binary components would be close to those derived using R between 4.0 and 4.1.

We also plotted the O5 V((f)) and O9.5 V components of FO 15 on a theoretical Hertzsprung-Russell (H-R) diagram (Figure 5) together with evolutionary tracks and stellar model calculations by A.M. Serenelli (private communication). Those models were computed using the stellar evolution code LPCODE described in Althaus et al. (2003). For the present calculations the mass loss rate is taken from de Jager et al. (1988).Overshooting was applied only for convective cores and the overshooting parameter adopted is $\alpha_{\rm over} = d_{\rm over} = 0.2$. As can be seen in Figure 5, both components of FO 15 lie to the left of the Zero Age Main Sequence (ZAMS) isochrone and near the 33 and 15 $M_\odot$ evolutionary tracks, respectively, similar to the masses derived using $R = 4.1$.

5 X-RAY ANALYSIS

In order to study the properties of the X-ray emission of FO 15 we used XMM-Newton data sets for revolutions #115 and #116 (see Table 1). We extracted individual PN and MOS pulse-height and background X-ray spectra, and we constructed the appropriate *Ancillary Response Files* (ARF) and *Redistribution Matrix Files* (RMF) using the ARFGEN and RMFGEN SAS v6.0.0 commands, respectively. We also

Table 4. Physical parameters of FO 15 (O5V((f)) + O9.5V) components for different values of the ratio of total to selective extinction (R).

Physical	R = 3.2		R = 3.5		R = 3.9		R = 4.0		R = 4.1		R = 4.2	
Parameters	Prim.	Sec.	Prim.	Sec.	Prim.	Sec.	Prim.	Sec.	Prim.	Sec.	Prim.	Sec.
A_v	3.81		4.16		4.64		4.76		4.87		4.99	
V_0	8.24		7.88		7.40		7.29		7.17		7.05	
M_v^{sys}	-3.52		-3.87		-4.35		-4.47		-4.59		-4.70	
M_v	-3.27	-1.77	-3.63	-2.12	-4.11	-2.60	-4.22	-2.72	-4.34	-2.84	-4.46	-2.96
M_{bol}	-7.14	-4.81	-7.49	-5.17	-7.97	-5.65	-8.09	-5.77	-8.20	-5.89	-8.32	-6.00
L_{bol} [$L_\odot$]	51500	6076	71500	8400	110900	13100	123600	14600	138000	16300	154000	18200
R_{sb} [$R_\odot$]	4.47	2.68	5.27	3.15	6.56	3.93	6.93	4.15	7.32	4.38	7.74	4.63
V_{sy} [km s^{-1}]	160	96	188	113	235	140	248	149	262	156	277	165
i [degrees]	—		—		—		82^{90}_{75}		70^{74}_{66}		63^{65}_{60}	
R_{rl} [$R_\odot$]	—	—	—	—	—	—	8.11	6.09	8.34	6.26	9.00	6.74
M [$M_\odot$]	—	—	—	—	—	—	28.8	15.5	33.7	18.1	39.6	21.2

The adopted effective temperatures and bolometric corrections are as follows: T_{eff}(O5V((f))) = 42000 K , BC_1(O5V) = -3.86 and T_{eff}(O9.5V) = 31850 K , BC_2(O9.5V) = -3.04. R_{sb} and V_{sy} refer to the Stefan-Boltzmann radii and rotational synchronous velocities, respectively. The Roche lobe radii were obtained using the expression given by Paczyński (1971).

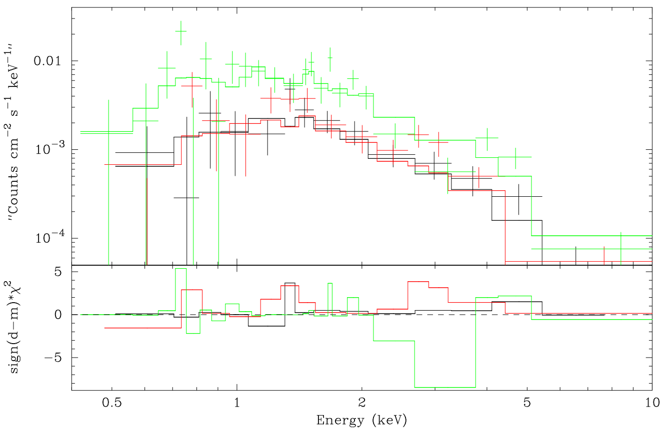

Figure 6. Observed EPIC (PN+MOS1+MOS2) multiple fitted spectrum of FO 15 form XMM-Newton revolution #115 data. We show a 2T MEKAL model affected by a combined multiplicative warm absorption law ($wabs_{ISM} \times wabs_{wind}$).

used the matrices provided by the XMM-Newton SOC, although no difference was found between the spectra obtained in each way.

Each EPIC source spectra was extracted in the 0.3 to 12 keV energy range, within a circular region of 15 arcsec centered at FO 15. The background was selected within an annular region with the same previous area, that means an outer radius $\sqrt{2}$ times larger than the source region. The spectra were binned to reach a minimum of 6 and 12 counts per channel for MOS 1/ 2 and PN 1 cameras, and the background corrected spectra were analyzed using the XSPEC software (version 11.3.1). Independent and simultaneous fits to the PN and MOS spectra were performed with consistent results.

Taking into account that the signal to noise ratio is about 4 times greater in the #115 than in the #116 revolution data set, the uncertainties of the derived parameters of the model, and the fact that the source is intrinsically variable, we decided to adopt only the data from revolution #115 in order to derive a model for the X-ray sepctrum of FO 15 .

From our extracted spectra we fitted single and multiple component models affected by multiplicative photoelectric energy-dependent absorption, based on cross-sections provided by Balucinska-Church & McCammon (1992). The importance of including *warm* absorption components in the analysis of the X-ray emission from OB stars has been emphasized, for example, by Waldron (1984). We considered a *warm* absorber model ($N_{wind} \times N_{ISM}$) in which the X-ray source is first attenuated by the stellar wind absorption (N_{wind}), followed by attenuation by the fixed observed ISM component (N_{ISM}). Following Shull & van Steenberg (1985) and adopting a E(B-V) = 1.20 (Forte & Orsatti 1981) we fixed the interstellar column of neutral hydrogen (N_{ISM}) to 0.62×10^{22} cm^{-2}.

We first tried a power-law model with a $\Gamma \approx 2.6$, which fits well the high energy tail observed in the FO 15 X-ray spectrum. This component has a much steeper slope than the value $\Gamma = 1.5$ expected for inverse Compton scattering emission by relativistic electrons accelerated in strong shocks (Chen & White 1991). But this model failed in producing an acceptable fit (the reduced χ^2 is 1.4 for 134 d.o.f., instead of the desirable 1.0) mostly due to the lack of coincidence in the soft X-ray energies. As a second step, we tried a single-thermal model MEKAL (Mewe et al. 1985) with kT = 2.9±0.5 keV, which did not provide a good fit to the soft energies either (reduced χ^2 = 1.2/133 d.o.f.). Our final fit used a two-temperature model of $kT_1 = 0.16\pm0.02$ and $kT_2 = 2.7\pm0.4$, achieving a reduced $\chi^2 = 1.0$ with 131 d.o.f. The parameters for each fit are listed in Table 5.

In Figure 6 we present the fitted PN, MOS 1 MOS 2 and spectrum and the residual model for FO 15. The OVIII 0.77 keV and MgXII 1.47 keV lines are probably present in this spectrum, causing larger residuals at their positions. However, the low signal-to-noise makes the detection of these features statistically uncertain. If confirmed, the presence of these lines could be indicative of a thermal origin for the X-ray emission of FO 15.

In order to obtain the X-ray vs. bolometric luminosity ratio for FO 15 , we assumed for this star a distance modulus

Table 5. Spectral models of FO 15 for XMM-Newton revolutions #115 and #116 data sets.

Model Id.	Red. χ^2/dof	N_{wind} (10^{22} cm^{-2})	kT / Γ keV/index	Norm. (Y)	Model predicted rate ($\times10^{-3}$) MOS1	MOS2	PN	X-ray Flux Abs.	Un-Abs.
# 115									
PL	1.4/134	$\approx10^{-8}$	2.6±0.1	8.2×10^{-5}	3.7±0.5	3.8±0.6	12.3±1.2	1.3×10^{-13}	3.2×10^{-13}
1 T	1.2/134	$\approx10^{-8}$	2.9±0.5	1.2×10^{-4}	3.5±0.5	3.6±0.6	11.4±1.2	1.2×10^{-13}	2.0×10^{-13}
2 T	0.96/131	0.18±0.1	0.16±0.02 2.7±0.4	7.0×10^{-4} 1.3×10^{-4}	4.7±0.5	5.8±0.6	13.2±1.2	1.2×10^{-13}	13.0×10^{-13}
# 116									
PL	1.5/52	$\approx10^{-4}$	3.4±1.4	5.7×10^{-5}	1.9±0.7	2.0±1.2	6.6±2.1	0.4×10^{-13}	2.9×10^{-13}
1 T	1.2/52	0.13±0.1	0.9±0.8	7.7×10^{-5}	1.8±0.9	1.8±1.1	6.2±2.1	0.3×10^{-13}	1.3×10^{-13}
2 T	1.1/47	0.53±0.4	0.40±0.30 2.5±1.3	1.6×10^{-4} 4.6×10^{-5}	2.1±0.9	2.1±1.1	7.2±2.1	0.5×10^{-13}	6.2×10^{-13}

Note: The best fit corresponds to the two temperature model $\mathrm{wabs_{ISM}.wabs_{wind}}$(mekal+mekal). The interstellar column density ($\mathrm{wabs_{ISM}}$) is frozen at 0.62×10^{22} (cm^{-2}) for all models. N_{wind} gives the equivalent ionized hydrogen column of absorbing matter in the stellar wind. kT is the temperature of the MEKAL component (in keV). The normalization parameter (Y) of the MEKA models is defined as $(10^{-14}/4\pi d^2)\int n_e n_H dV$, where d, n_e and n_H are respectively the distance to the source in (cm), the electron and hydrogen densities in (cm^{-3}). For the power law the Norm parameter corresponds to the photon flux at 1 keV. The errors refer to the 1σ confidence level.

of 11.76 ± 0.15 (2250 ± 180 pc) Davidson et al. (2001), which gives for the system a bolometric luminosity of $L_{bol} = 6.02\times10^{38}$ erg s^{-1}. Furthermore, the unabsorbed X-ray luminosities for the # 115 and # 116 revolution data sets are $L_X^0 = 7.87\times10^{32}$ and 3.63×10^{32} erg s^{-1}, which produces luminosity ratios of $L_x/L_{bol} \approx 1.3\times10^{-6}$ and 6.0×10^{-7}, respectively. The first value is about 2 times greater than the second, while this last is in agreement with that obtained by Albacete Colombo et al. (2003) for most O-type stars in the Carina Nebula region.

The excess in the observed X-ray flux for revolution #115, could be denoting pahe-locked variations of the X-ray emission of FO 15 probably originated in colliding winds. In a forthcoming paper we shall use a wider set of X-ray observations in order to study the X-ray spectrum of FO 15 at different phases of the binary motion, as well as the short and long term behavior of the X-ray emission from this star.

6 SUMMARY AND CONCLUSIONS

In this paper we have demonstrated that FO 15 is a double-lined spectroscopic binary with a period of 1.41358 ± 0.00001 days. From low and high resolution spectra of FO 15 we measured radial velocities and derived a circular orbtial solution for the system with semiamplitudes of 231 ± 3 and 423 ± 9 km s^{-1}, for the primary and secondary components, respectively. The corresponding minimum masses are 28 and 15 $M_\odot$.

Also, using our high resolution spectra we have classified the spectrum of the primary and secondary components of FO 15 as O5 V((f)) and O9.5 V, following the criteria proposed by Conti 1973 and Kerton et al. 1999. Visual comparison of the low and high resolution observations with the standard stars in the atlas by Walborn & Fitzpatrick (1990) was also performed arriving to coincident results. This spectral classification makes FO 15 the second earliest type double lined binary studied in the Carina Region, following HD 93205.

Physical parameters for the binary components of FO 15 have been derived under the assumpition of synchronous rotation, adopting for the system de distance modulus derived by Davidson et al. (2001) for Eta Carinae, and for different values of the ratio of the selective to total absorption parameter R. Our best guess is for R=4.1, yielding for the O5V((f)) and O9.5V components, masses of 33.7 and 18.1 and radii of 8.3 and 6.3, expressed in solar units.

We also placed the components of FO 15 on a theoretical H-R diagram along with isochrones and evolutionary tracks from Althaus et al. (2003). Both components lie to the left of the ZAMS isochrone, and near the evolutionary tracks of 33 and 15 $M_\odot$, respectively, in good agreement with the extreme youth of the system and the high dynamical masses.

FO 15 was observed by XMM-Newton with the EPIC cameras, revealing an anomalous hard X-ray spectrum of about kT ≈ 2.7 keV (3.1×10^7 K), and a real overluminosity $L_x/L_{bol} \approx 1.3\times10^{-6}$, two times greater in the #115 than #116 X-ray observation. This behavior can be originated in wind-wind interaction in this hot, luminous, and short period system. We found also evidence of short term and long phase locked variability in the X-ray emission, which will be discussed in a forthcoming paper.

A photometric study of FO 15 is under way (Fernández Lajús et al. in preparation). Once a light curve is derived, simultaneous analysis with the radial velocities presented in this paper will provide absolute values for the masses and radii of the binary components that will confirm or correct our present derivations.

FO 15 deserves extensive followup as a consquence of its very hot components, its short age (its components are good candidates to belong to the Zero Age Main Sequence of Trumpler 16) and the evidence of wind-wind interaction which follows from the characteristics of its X-ray emission. It is also surrounded by dense insterstellar material best represented by an anomalous R value. In summary, FO 15 is a key system for the study of massive star characteristics and evolution, including tests of the behavior of colliding winds.

7 ACKNOWLEDGMENTS

We are indebted to Roberto Gamen for kindly obtaining 2 spectra of FO15 for this study. We thank A.M. Serenelli for making available the evolutionary model calculations used in this paper. We thank the Director and staff of CASLEO for the use of their facilities, and acknowledge the use, at CASLEO, of the CCD and data acquisition system supported under US NSF grant AST-90-15827 to R.M. Rich. NM is grateful to the director and staff of Las Campanas Observatory for technical support and kind hospitality.

REFERENCES

Albacete Colombo J. F., Méndez M., Morrell N. I., 2003, Mon. Not. R. Astron. Soc., 346, 704
Althaus L. G., Serenelli A. M., Córsico A. H., Montgomery M. H., 2003, Astron. Astrophys., 404, 593
Auer L. H., Mihalas D., 1972, Astrophys. J., Suppl. Ser., 24, 193
Balucinska-Church M., McCammon D., 1992, Astrophys. J., 400, 699
Bernstein R., Shectman S. A., Gunnels S. M., Mochnacki S., Athey A. E., 2003, in Instrument Design and Performance for Optical/Infrared Ground-based Telescopes. Edited by Iye, Masanori; Moorwood, Alan F. M. Proceedings of the SPIE, Volume 4841, pp. 1694-1704 (2003). MIKE: A Double Echelle Spectrograph for the Magellan Telescopes at Las Campanas Observatory. pp 1694–1704
Bertiau F. C., Grobben 1969 A Program for the Determination of the Orbital Elements of Spectroscopic Binaries. Ric. Astronom. Sp. Vaticana, **8**, 1.
Bolton C. T., Rogers G. L., 1978, Astrophys. J., 222, 234
Chen W., White R. L., 1991, Astrophys. J., 366, 512
Chlebowski T., Harnden F. R., Sciortino S., 1989, Astrophys. J., 341, 427
Cincotta P. M., Méndez M., Nuñez J. A., 1995, Astrophys. J., 449, 231
Conti P. S., 1973, Astrophys. J., 179
Conti P. S., Alschuler W. R., 1971, Astrophys. J., 170, 325
Corcoran M. F., 1996, in Workshop on Colliding Winds in Binary Stars to Honor Jorge Sahade, vol. 5 X-Ray Emission From Colliding Wind Binaries. p. 54
Davidson K., Smith N., Gull T. R., Ishibashi K., Hillier D. J., 2001, Astron. J., 121, 1569
de Jager C., Nieuwenhuijzen H., van der Hucht K. A., 1988, Astron. Astrophys. Suppl. Ser., 72, 259
Forte J. C., Orsatti A. M., 1981, Astron. J., 86, 209
Grabelsky D. A., Cohen R. S., Bronfman L., Thaddeus P., 1988, Astrophys. J., 331, 181
Herrero A., Kudritzki R. P., Vilchez J. M., Kunze D., Butler K., Haser S., 1992, Astron. Astrophys., 261, 209
Herrero A., Puls J., Villamariz M. R., 2000, Astron. Astrophys., 354, 193
Howarth I. D., Prinja R. K., 1989, Astrophys. J., Suppl. Ser., 69, 527
Kerton C. R. Ballantyne D. R., Martin P. G., 1999, Astron. J., 117, 2485
Lafler J., Kinman T. D., 1965, Astrophys. J., Suppl. Ser., 11, 216
Markova N., Puls J., Repolust T., Markov H., 2004, Astron. Astrophys., 413, 693
Marraco H. G., Muzzio J. C., 1980, Publ. Astron. Soc. Pac., 92, 700
Massey P., Johnson J., 1993, Astron. J., 105, 980
Mathys G., 1988, Astron. Astrophys. Suppl. Ser., 76, 427
Mewe R., Gronenschild E. H. B. M., van den Oord G. H. J., 1985, Astron. Astrophys. Suppl. Ser., 62, 197
Paczyński B., 1971, Ann. Rev. Astron. Astrophys., 9, 183
Petrie R. M., 1940, Publications of the Dominion Astrophysical Observatory Victoria, 7, 245
Schmidt-Kaler T., 1982, Landolt-Börnstein, 2, 455
Shull J. M., van Steenberg M. E., 1985, Astrophys. J., 294, 599
Strüder L. e. a., 2001, Astron. Astrophys., 365, L18
Tapia M., Roth M., Marraco H., Ruiz M. T., 1988, Mon. Not. R. Astron. Soc., 232, 661
Tapia M., Roth M., Vázquez R. A., Feinstein A., 2003, Mon. Not. R. Astron. Soc., 339, 44
Turner M. J. L. e. a., 2001, Astron. Astrophys., 365, L27
Walborn N. R., Fitzpatrick E. L., 1990, Publ. Astron. Soc. Pac., 102, 379
Waldron W. L., 1984, Astrophys. J., 282, 256
Zahn J.-P., 1977, Astron. Astrophys., 57, 383